Re-evaluating the reactive uptake of HOBr in the troposphere with implications for the marine boundary layer and volcanic plumes

Tjarda J. Roberts[1], Line Jourdain[1], Paul T. Griffiths[2], and Michel Pirre[1]

[1] {LPC2E, UMR 7328, CNRS-Université d'Orléans, 3A Avenue de la Recherche Scientifique, 45071 Orleans, Cedex 2, France}

[2] {Centre for Atmospheric Science, Cambridge University, Chemistry Department, Lensfield Road, Cambridge, CB2 1EW, UK}

Correspondence to: T. J. Roberts (Tjarda.Roberts@cnrs-orleans.fr)

Abstract

The reactive uptake of HOBr onto halogen-rich aerosols promotes conversion of $Br^-_{(aq)}$ into gaseous reactive bromine (incl. BrO) with impacts on tropospheric oxidants and mercury deposition. However, experimental data quantifying HOBr reactive uptake on tropospheric aerosols is limited, and reported values vary in magnitude. This study introduces a new evaluation of HOBr reactive uptake coefficients in the context of the general acid assisted mechanism. We emphasise that the termolecular kinetic approach assumed in numerical model studies of tropospheric reactive bromine chemistry to date is strictly only valid for a specific pH range and, according to the general acid assisted mechanism for HOBr, the reaction kinetics becomes bimolecular and independent of pH at high acidity.

This study reconciles for the first time the different reactive uptake coefficients reported from laboratory experiments. The re-evaluation confirms HOBr reactive uptake is rapid on moderately acidified sea-salt aerosol (and slow on alkaline aerosol), but predicts very low reactive uptake coefficients on highly-acidified submicron particles. This is due to acid-saturated kinetics combined with low halide concentrations induced by both acid-displacement reactions and the dilution effects of $H_2SO_{4(aq)}$. A mechanism is thereby proposed for reported Br-enhancement (relative to Na) in H_2SO_4-rich submicron particles in the marine environment. Further, the fact that HOBr reactive uptake on H_2SO_4-acidified supra-micron particles is driven by HOBr+Br- (rather than HOBr+Cl-) indicates self-limitation via decreasing γ_{HOBr} once aerosol Br- is converted into reactive bromine.

First predictions of HOBr reactive uptake on sulphate particles in halogen-rich volcanic plumes are also presented. High (accommodation limited) HOBr+Br^- uptake coefficient in concentrated (> 1 µmol/mol SO_2) plume environments supports potential for rapid BrO formation in plumes throughout the troposphere. However, reduced HOBr reactive uptake may reduce the rate of BrO cycling in dilute plumes in the lower troposphere.

In summary, our re-evaluation of HOBr kinetics provides a new framework for interpretation of experimental data and suggests the reactive uptake of HOBr on H2SO4-acidifed particles is substantially over-estimated in current numerical models of BrO chemistry in the troposphere.

1. Introduction

The reactive uptake of HOBr onto halogen-containing aerosols to release Br_2 enables propagation of the chain reaction leading to autocatalytic BrO formation, the so-called 'bromine explosion', (Vogt et al., 1996), first proposed following the discovery of ozone depletion events in the polar boundary layer (Barrie et al. 1988). Rapid and substantial (10's ppbv) ozone depletion occurs upon the formation of just 10's pptv BrO due to cycling between Br and BrO, with further Br-mediated impacts on environmental mercury in the conversion of Hg^0 to more reactive and easily deposited form Hg^{II} (Schroeder et al., 1998). Tropospheric BrO chemistry has since been recognised outside the polar regions, with BrO identified above salt pans (Hebestreit et al., 1999), in the marine boundary layer (Read et al. 2008), and is suggested to have a significant impact on the chemistry of the free troposphere (e.g. von Glasow et al., 2004). In particular, recent evidence of rapid BrO formation in acidic volcanic plumes (10's pptv to ppbv on a timescale of minutes) has highlighted volcanic halogen emissions as a source of reactive bromine entering the troposphere (Bobrowski et al., 2003).

R1 $HOBr_{(g)} \rightarrow HOBr_{(aq)}$

R2 $HOBr_{(aq)} + Br^-_{(aq)} + H^+_{(aq)} \rightarrow Br_{2(aq)} + H_2O_{(l)}$

R3 $HOBr_{(aq)} + Cl^-_{(aq)} + H^+_{(aq)} \rightarrow BrCl_{(aq)} + H_2O_{(l)}$

R4 $BrCl_{(aq)} + Br^-_{(aq)} \leftrightarrow Br_2Cl^-_{(aq)} \leftrightarrow Br_{2(aq)} + Cl^-_{(aq)}$

R5 $Br_{2(aq)} \leftrightarrow Br_{2(g)}$

R6 $Br_{2(g)} \xrightarrow{h\nu} 2Br_{(g)}$

R7 $2Br_{(g)} + 2O_{3(g)} \rightarrow 2BrO_{(g)} + 2O_{2(g)}$

R8 $2BrO_{(g)} + 2HO_{2(g)} \rightarrow 2HOBr_{(g)} + 2O_{2(g)}$

Key to reactive halogen formation is the cycle R1-R8 which results in autocatalytic formation of BrO. Accommodation of $HOBr_{(g)}$ to aerosol (R1), followed by reaction with $Br^-_{(aq)}$ or $Cl^-_{(aq)}$ and $H^+_{(aq)}$ results in a di-halogen product (R2,R3). The reaction of HOBr with $Cl^-_{(aq)}$ (R3) is typically considered the dominant reaction pathway (albeit an assumption that may not apply in highly acidified aerosol as

we show in this study) given sea-salt aerosol contains $[Br^-_{(aq)}] << [Cl^-_{(aq)}]$ by a factor of 700 (or greater once reactive bromine formation has commenced), and the termolecular rate constants for R2 and R3 are of comparable magnitudes (Liu and Margarem, 2001, Beckwith et al., 1996). However, Br_2 is commonly the observed product, as confirmed by laboratory experiments by Fickert et al. (1999). The product conversion from BrCl to Br_2 is explained by aqueous-phase equilibria (R4) that interconvert BrCl into Br_2 (via Br_2Cl^-) before gaseous release (R5). According to equilibrium constants reported by Wang et al. (1994), conversion of BrCl to Br_2 is favoured at room temperature in aerosol provided $Br^-_{(aq)}:Cl^-_{(aq)} > \sim 10^{-4}$, as for example in sea-salt aerosol where $Br^-_{(aq)}:Cl^-_{(aq)} \approx 1.5 \cdot 10^{-3}$. The dihalogen species then partition into the gas-phase, R5. The exsolution of dihalogens from the aerosol to the gas-phase also limits the occurrence of reverse reactions that might reform HOBr. Once in the gas-phase, Br_2 is photolysed to produce 2 Br radicals, R6, which may react with ozone to form BrO, R7. HOBr is reformed via the reaction of BrO with HO_2, (R8), whereupon it may react again with halogen-containing aerosol to further propagate the cycle, each time doubling the concentration of reactive bromine.

Numerical models have been developed to better understand the formation of BrO and evaluate impacts on atmospheric oxidants throughout the troposphere and on mercury cycling in the environment. Models capture the salient features of BrO formation and impacts (e.g. on ozone depletion and Hg deposition events) in the different tropospheric environments (for reviews by Simpson et al. 2007 and Saiz-Lopez A. and von Glasow R., 2012). Nevertheless, a number of uncertainties remain. For example, models tend to overestimate Br_x cycling in the marine environment (Sander et al., 2003; Smoydzin and von Glasow, 2007; Keene et al., 2009). Models predict a depletion in the inorganic bromine content of all acidified marine aerosols, as consequence of HOBr reactive uptake to form Br_2 and its release into the gas-phase. However, an aerosol bromine deficit is only observed in the slightly acidified supramicron fraction, whislt aerosol bromine is found to be enhanced (relative to that expected based on Br:Na ratios in sea-salt, using sodium as a sea-salt tracer) in the highly acidified sub-micronmeter fraction. This phenomenon has not been explained to date (Sander et al., 2003). Numerical models have also attempted to simulate reactive halogen chemistry in volcanic plume environments. Models initialised with a high-temperature source region, are able to reproduce the rapid formation of BrO in the near-source plume (Bobrowski et al. , 2007a, Roberts et al., 2009, Von Glasow 2010), as well as ozone depletion (Kelly et al., 2013), but a source of model uncertainty is the representation of heterogeneous halogen

chemistry on volcanic aerosol, which may differ from that reported from experiments on sea-salt aerosol.

All these studies rely on laboratory experiments to quantify rate constants of the reactions, with a key process in the formation of reactive bromine being the reaction of $HOBr_{(aq)}$ with halide ion $X^-_{(aq)}$ ($Cl^-_{(aq)}$ or $Br^-_{(aq)}$) and $H^+_{(aq)}$, R2,R3, which can be written generically as R9.

R9 $$HOBr_{(aq)} + H^+_{(aq)} + X^-_{(aq)} \xrightarrow{k_{ter}, k^{II}, k^{I}} BrX_{(aq)} + H_2O_{(aq)}$$

Experimental studies (e.g. Fickert et al., 1999) show the reaction of $HOBr_{(aq)}$ is promoted when alkaline sea-salt aerosols becomes acidified, either by natural (e.g. methane sulphonic acid) or anthropogenic (e.g. sulphuric acid) sources of acidity. However, laboratory experiments have reported uptake coefficients on acidified sea-salt aerosol, >0.2 (Abbatt and Wachewsky, 1998) and 10^{-2} (Pratte and Rossi, 2006), a discrepancy that has not been explained to date. In addition, no experiments have been performed to quantify uptake of HOBr on volcanic aerosol under tropospheric conditions.

Numerical model studies of reactive bromine chemistry currently implement R9 using three-body reaction kinetics, i.e. assumed the reaction rate is directly proportional to $H^+_{(aq)}$ concentration (e.g. von Glasow, 2002), or using uptake coefficients calculated on this assumption (IUPAC evaluations, e.g. Ammann et al., 2013). We highlight, however, that earlier literature on the general acid-assisted mechanism for this and similar reactions (e.g. Eigen and Kustin, 1962, Nagy et al., 1988) identify that the pH dependence of the reaction rate is more complex, with acid-saturation of the kinetics at high acidity.

This study re-evaluates HOBr reactive uptake in the context of the general acid assisted mechanism for the first time. The plan of the paper is as follows. In Section 2 the method for calculating the reactive uptake coefficient is recalled with the approach based on the general acid assisted mechanism explained. The data used to evaluate the new uptake coefficient calculations are presented. In Section 3 pH-dependent second-order rate constants (k^{II}) are derived for both $HOBr+Br^-$ and $HOBr+Cl^-$ in the context of the general assisted mechanism, using reported literature data for the underlying rate constants, and a thermodynamic model to predict aerosol composition under experimental conditions. Using the new parameterisation for k^{II}, reactive uptake coefficients for HOBr + Br- and HOBr + Cl- are calculated and compared to reported laboratory data for HCl-acidified sea-salt aerosol (Wachewsky and Abbatt, 1998) and H_2SO_4-acidified sea-salt aerosol (Pratte and Rossi, 2006). We provide new quantification of $HOBr+Br^-$ and $HOBr+Cl^-$ uptake coefficients on H_2SO_4-acidified sea-salt aerosol in the marine environment, and sulphuric acid aerosol in volcanic

plumes dispersing into the troposphere. In section 4, reactive uptake coefficients are calculated for HOBr on H_2SO_4-acidified sea-salt aerosol in the marine environment, and on sulphuric acid aerosol in volcanic plumes entering the troposphere, and implications discussed for BrO chemistry in these environments.

2. Method and experimental data

2.1 Quantifying the reactive uptake coefficient, γ_{HOBr}

The reactive uptake of $HOBr_{(g)}$ can be quantified by E1 (with further modification required for large particles due to the limitation of gas-phase diffusion) in terms of the reactive uptake coefficient, γ_{HOBr}, where v_{HOBr}, is the mean molecular velocity of $HOBr_{(g)}$, cm s^{-1}, and *Area*, is the surface area density of the aqueous phase, cm^2/cm^3.

γ_{HOBr} is a fractional number that quantifies the likelihood of reaction given a collision of $HOBr_{(g)}$ with a particle, and can be calculated following the resistor-model framework (E2) that describes the accommodation to the aerosol, and the reaction and diffusion in or across the aerosol particle. γ_{HOBr} is a function of several parameters, including accommodation coefficient, α_{HOBr}, the solubility of HOBr, H^*, the aqueous-phase diffusion rate, D_l, the gas constant R, Temperature, T, the mean molecular velocity, v_{HOBr}, and the first-order rate constant for the reaction of $HOBr_{(aq)}$, k^I. The parameter *l* is a function of D_l and k^I, $l = (D_l/k^I)^{0.5}$.

E1 $$-\frac{d[HOBr_{(g)}]}{dt} = \gamma_{HOBr} \cdot \frac{v_{HOBr}}{4} \cdot [HOBr_{(g)}] \cdot Area$$

E2 $$\frac{1}{\gamma_{HOBr}} = \frac{1}{\alpha_{HOBr}} + \frac{v_{HOBr}}{4 \cdot H^*_{HOBr} \cdot R \cdot T \cdot \sqrt{D_{l,HOBr} \cdot k^I}} \cdot \frac{1}{\coth\left[\frac{r}{l}\right] - \frac{l}{r}}$$

E3 $$-\frac{d[HOBr_{(aq)}]}{dt} = k^I \cdot [HOBr_{(aq)}]$$

E4 $$k^I = k_{ter} \cdot [X^-_{(aq)}] \cdot [H^+_{(aq)}]$$

E5 $$k^I = k^{II} \cdot [X^-_{(aq)}]$$

To date, numerical models have adopted two approaches to simulate the reactive uptake of HOBr. Detailed process models (e.g. MISTRA; von Glasow et al. (2002), MECCA; Sander et al. (2011)) tend to model HOBr gas-aerosol partitioning to and from the aerosol directly, with the reaction of HOBr

inside the aerosol simulated using E3 and termolecular kinetics (E4). On the other hand, global models (e.g. in studies by von Glasow et al., (2004), Yang et al., (2005), Breider et al., (2010), Parella et al. (2012)) tend to simulate HOBr reactive uptake as one step, E1, quantified by the uptake coefficient, γ_{HOBr}. The IUPAC evaluation recommends uptake coefficient to be calculated using E2 and the termolecular approach to HOBr kinetics, E4. In global models, a fixed uptake coefficient, γ_{HOBr}, is typically used for computational reasons.

However, as we highlight in this study, the termolecular kinetics approach (E4) is only valid within a limited pH range. Here we instead use E2 and the reaction kinetics of $HOBr_{(aq)}$ in terms of a second-order rate constant, E5, where k^{II} is a variable function of pH according to the general acid assisted reaction mechanism for $HOX+Y^-$ ($+H^+$) constrained by available laboratory data. Details on the mechanism and derivation of k^{II} are given in Section 1 of Supplementary maertial and Section 3.1). Despite being well-documented (Eigen and Kustin, 1962; Kumar and Margarem, 1987; Nagy et al. 1988; Gerritsen and Margarem, 1990, Wang and Margarem, 1994) this mechanism has not been implemented in any numerical model studies of reactive halogen chemistry to date.

To calculate reactive uptake coefficients (E2), we also need to determine the aerosol composition, specifically halide concentration, $[X^-_{(aq)}]$ and the acidity. Indeed, $[X^-_{(aq)}]$ is needed for E5 and subsequently E2 , and the acidity is also needed to determine k^{II} in the context of the general assisted mechanism (see the expression in Section 3.1) and subsequently E5 and E2. This was achieved using the E-AIM (Extended- Aerosol Inorganic model) and Henry's constants (for more details see Section 3 of Supplementary Material). Given high ionic strength of the solutions studied, concentrations were converted to activities using activity coefficients provided by E-AIM.

Finally, we assume in E2 an accommodation coefficient of 0.6 (Wachsmuth et al., 2002), with solubility and diffusion coefficients for HOBr in water and sulphuric acid derived from Frenzel et al. (1998), Iraci et al. (2005), and Klassen et al (1998). A radius of 0.1 or 1 um was assumed, reflecting the presence of both sub- and supra-micron particles in volcanic and marine environments. Further details are provided in Section 2 of Supplementary Materials.

We compare our new approach to reported estimates of HOBr reactive uptake coefficients from laboratory experiments as outlined below.

2.2 Reported experimental studies on the reactive uptake of HOBr onto liquid aerosol

A number of laboratory experiments (Table 1) have quantified the reactive uptake of HOBr onto acidified sea-salt aerosol under tropospheric conditions (as well as on solid particles, not considered

here). The accommodation coefficient for HOBr onto super-saturated $NaBr_{(aq)}$ aerosol was determined by Wachsumth et al. (2002) to be $\alpha_{HOBr} = 0.6 \pm 0.2$ at 298 K.

Experiments using acidified sea-salt particles made by nebulizing a 5 M NaCl and 0.5 M HCl solution under conditions representative of the troposphere found the reactive uptake coefficient for the reaction (HOBr+Cl-) to be very high ($\gamma_{HOBr} > 0.2$) on deliquesced aerosol (RH > 75%, T = 298 K), (Abbatt and Waschewsky, 1998). Conversely, experiments by Pratte and Rossi (2006) on H_2SO_4-acidified sea-salt aerosol with H_2SO_4:NaCl molar ratio = 1.45:1 at 296 K measured a substantially lower HOBr uptake coefficient, $\gamma_{HOBr} \sim 10^{-2}$, with a dependence on relative humidity ($\gamma_{HOBr} \sim 10^{-3}$ below 70% RH). This large (10^1-10^2) discrepancy has not been resolved to date. Uptake of HOBr on pure sulfate aerosol at 296 K is found to be low ($\gamma_{HOBr} \sim 10^{-3}$), Pratte and Rossi (2006).

Aqueous-phase rate constants for the reaction of $HOBr+X^-+H^+$ have also been reported: for $HOBr+Br^-_{(aq)}$, Eigen and Kustin (1952) and Beckwith et al. (1996) report termolecular rate constants of $k_{ter} = 1.6 \cdot 10^{10}$ M^{-2} s^{-2} over a pH range of 2.7-3.6 and 1.9-2.4 at 298 K, respectively. For $HOBr+Cl-_{(aq)}$, Liu and Margarem (2001) report a three-body rate constant of $2.3 \cdot 10^{10}$ M^{-2} s^{-2} in buffered aerosol at pH = 6.4 and 298K. Pratte and Rossi (2006) derived first-order rate constants for the reaction of $HOBr_{(aq)}$ from their uptake experiments, finding $k^I \sim 10^3$ s^{-1}.

The IUPAC subcommittee for gas kinetic data evaluation currently recommends an uptake coefficient parameterisation utilising accommodation coefficient α_{HOBr}= 0.6 (Wachsmuth et al., 2002), and first-order rate constant $k^I = k_{ter} \cdot [H^+_{(aq)}] \cdot [X^-_{(aq)}]$, with $k_{ter} = 2.3 \cdot 10^{10}$ M^{-2} s^{-1} (Liu and Margarem, 2001) for $HOBr+Cl^-$ and $k_{ter} = 1.6 \cdot 10^{10}$ M^{-2} s^{-1} (Beckwith et al., 1996) for $HOBr+Br^-$. Assuming a $Cl^-_{(aq)}$ concentration of 5.3 M typical of sea-water and low uptake coefficients in alkaline sea-salt aerosol (IUPAC evaluation, see website, e.g. Ammann et al., 2013), this parameterisation yields a high uptake coefficient, $\gamma_{HOBr} \sim 0.6$, on acidified sea-salt aerosol, and is in agreement with $\gamma_{HOBr} \geq 0.2$ reported by Abbatt and Waschewsky (1998) while overestimating the uptake coefficient as reported by Pratte and Rossi (2006) by a factor of ~20.

Here we present new uptake calculations based on the general acid assisted mechanism rather than termolecular kinetics in an attempt to consolidate these contrasting reported uptake coefficients within a single framework for the first time, and explain differences between model predictions and field observations of reactive bromine in the marine environment, as well as making first predictions of HOBr reactive uptake coefficients in volcanic plumes.

3 Results

3.1 The second-order rate constant for aqueous-phase reaction of HOBr with halide ions

In the general acid-assisted mechanism - whereby the rate of reaction of $HOBr_{(aq)}$ (needed in E2) follows a second-order kinetics – an equilibrium is established between $HOBrX^-_{(aq)}$ and HOBr according to the rate constants of R10 and R11, k_1 and k_{-1} (Eigen and Kustin, 1962). The formation of products, R12, involves a transition-state, $[H_2OBrX_{(aq)}]^{TS}$ that is stabilised by proton-donation to the oxygen, with overall rate constant k_H. Moreover, formation of products can also occur at low acid concentrations via a slower pathway, R13, followed by fast reaction R14, with overall rate constant k_0.

R10 $$HOBr_{(aq)} + X^-_{(aq)} \xrightarrow{k_1} HOBrX^-_{(aq)}$$

R11 $$HOBrX^-_{(aq)} \xrightarrow{k_{-1}} HOBr_{(aq)} + X^-_{(aq)}$$

R12 $$HOBrX^-_{(aq)} + H^+_{(aq)} \xrightarrow{k_H \cdot [H_2OBrX_{(aq)}]^{TS}} H_2O_{(aq)} + BrX_{(aq)}$$

R13 $$HOBrX^-_{(aq)} \xrightarrow{k_0} OH^-_{(aq)} + BrX_{(aq)}$$

R14 $$OH^-_{(aq)} + H^+_{(aq)} \xrightarrow{fast} H_2O_{(aq)}$$

According to R10-R14, the rate of reaction of $HOBr_{(aq)}$ can be quantified in terms of a 2nd order rate constant (following E3 and E5) where k^{II} is a function of pH, as described by equation E6, whose derivation is provided in Supplementary Material.

E6 $$k^{II} = \frac{k_1 \cdot \left(k_0 + k_H \cdot [H^+_{(aq)}]\right)}{k_{-1} + k_0 + k_H \cdot [H^+_{(aq)}]}$$

In the limits of high and low acidity (E7 and E8), k^{II} is independent of aerosol acidity. For a mid-range acidity ($k_H \cdot [H^+_{(aq)}] << k_{-1}+k_0$), k^{II} becomes linearly dependent on $[H^+_{(aq)}]$ i.e. is acid-dependent (E9). In this mid-acidity regime (only), the acid-dependence is equal to the three-body or termoleuclar rate constant, $k_1 \cdot k_H/(k_{-1}+k_0) = k_{ter}$.

E7 $k^{II} = k_1$ at high acidity (the limit as $H^+_{(aq)}$ tends to infinity)

E8 $$k^{II} = \frac{k_1 \cdot k_0}{k_{-1} + k_0}$$ at very low acidity (the limit as $H^+_{(aq)}$ tends to zero)

247 E9 $$k^{II} = \frac{k_1 \cdot k_0}{k_{-1} + k_0} + \frac{k_1 \cdot k_H \cdot [H^+_{(aq)}]}{k_{-1} + k_0}$$

248 Equations E6-E9 describe k^{II} in terms of four underlying rate constants (k_1, k_{-1}, k_0, k_H) and the aerosol
249 acidity. However, quantifying these underlying rate constants using published data is somewhat
250 challenging given the limited experimental data. This is now attempted below.

251

252 **3.2 Estimating the underlying rate constants (k_1, k_{-1}, k_0, k_H) for HOBr+Br- and HOBr+Cl-**

253 A number of aqueous-phase rate constants for the reaction of $HOBr+X^-+H^+$ have been reported: For
254 $HOBr+Br^-_{(aq)}$, Eigen and Kustin (1952) and Beckwith et al. (1996) report termolecular rate constants
255 of k_{ter} = $1.6 \cdot 10^{10}$ M^{-2} s^{-2} over a pH range of 2.7-3.6 and 1.9-2.4 at 298 K, respectively. These
256 experiments quantified the rate of reaction in the termolecular regime only, although Eigen and
257 Kustin (1962) used a consideration of relative stability constants (e.g. for equilibrium molarity of
258 ternary compounds X_3^- or X_2OH^- relative to X^-, X_2 or XOH) across the halogen series: HOCl+Cl,
259 HOBr+Br and HOI+I to attempt to estimate underlying rate constants.

260 Using the reported experimental data, k^{II} parameterisations (in terms of the underlying rate
261 constants (k_1, k_{-1}, k_0 and k_H) and acidity according to E6 derived above) are estimated as follows.

262

263 **3.2.1 HOBr+Br-**

264 For $HOBr+Br^-$, Eigen and Kustin (1962), proposed order of magnitude estimates of $k_1 = 5 \cdot 10^9$ M^{-1} s^{-1},
265 $k_{-1} = 5 \cdot 10^9$ s^{-1}, $k_H = 2 \cdot 10^{10}$ M^{-1} s^{-1}, and $k_0 = 10^4$ s^{-1}. However, in Figure 4 of Beckwith et al. (1996), there
266 are indications of acid-saturation in their k^{II} rate constant data for $HOBr+Br^-$, seen as curvature in the
267 plots of observed k^{II} versus acidity. This is also seen in their Figure 5 where $k^{II}_{observed} \geq 2.3 \cdot 10^8$ M^{-1} s^{-1}.
268 We therefore suggest acid-saturation of the reaction between HOBr and Br^- may limit k^{II} to ~ $5 \cdot 10^8$
269 M^{-1} s^{-1}. We also adjust k_{-1} to $k_{-1} \sim 5 \cdot 10^8$ s^{-1} on the basis of the reported stability constant $k_1/k_{-1} \sim 1$ M^{-1}
270 (Eigen and Kustin, 1962). While, any evidence for acid-saturation lays within the reported error bars
271 for the data points this adjustment does not affect our general conclusions about $\gamma_{HOBr+Br}$ in this
272 study.

273

274 **3.2.1 HOBr+Cl-**

For $HOBr+Cl^-_{(aq)}$, Liu and Margarem (2001) report a three-body rate constant of $2.3\cdot10^{10}$ M^{-2} s^{-2} in buffered aerosol at pH = 6.4 and 298K. Pratte and Rossi (2006) also derived estimates for first-order rate constants for reaction of $HOBr_{(aq)}$ from their uptake coefficient experiments. We re-evaluate these data below to improve quantification of the reaction kinetics of $HOBr+Cl^-$.

For HOBr+Cl- , the underlying rate constants (k_1, k_{-1}, k_H, k_0) are estimated as follows. The rate constant k_1 is derived from the estimation of k^{II} at acid saturation (E7). For this, we estimated k^{II} at pH -1 to 0 from experiments of Pratte and Rossi (2006), Table 2. These new estimates of k^{II} are derived from first order k^I rate constants for the reaction of $HOBr_{(aq)}$, reported by Pratte and Rossi (2006), where $[Cl^-_{(aq)}]$ is calculated by the E-AIM model from experimental conditions, E-AIM predicts chloride concentrations are reduced under the experimental conditions as consequence of acid-displacement of $HCl_{(g)}$ (see further discussion in Supplementary Material). We find k^{II} ~10^4 M^{-1} s^{-1} over pH -1 to 0, see Table 2 for details. We note that in their reporting of k^I rate constants from their uptake experiments, Pratte and Rossi, (2006) assumed an accommodation coefficient of either α_{HOBr} = 0.2 or α_{HOBr} = 0.02. Given that experiments on $NaBr_{(aq)}$ aerosol have identified an accommodation coefficient for HOBr on $NaBr_{(aq)}$ particles of 0.6 (Wachsmuth et al. 2002), the k^{II} data derived assuming α_{HOBr}=0.2 are likely more representative. Nevertheless, either case yields estimate for k^{II} ~ 10^4 M s^{-1} over pH = 0 to-1. A second estimate for k^{II} is made from the reported three-body rate constant of $2.3\cdot10^{10}$ M^{-2} s^{-2} at pH = 6.4, by setting $k^{II} = k_{ter}\cdot[H^+_{(aq)}]$. This yields $k^{II} = 9\cdot10^3$ M^{-1} s^{-1} at pH 6.4.

Thus, collectively these two datasets at pH = 6.4 and 0 to -1 suggest that k^{II} is acid saturated at ~10^4 M s^{-1} at pH ≤ 6. Based on this value for k^{II} at acid saturation (where $k^{II} = k_1$) we set $k_1 = 1.2\cdot10^4$ M s^{-1}, as an average estimate, which is less than k_1 for $HOBr+Br^-$, and which is consistent with the greater nucleophile strength of Br^- compared to Cl^-. We fix $k_H = 2\cdot10^{10}$ M^{-1} s^{-1} , equal to that estimated by Eigen and Kustin (1961) for $HOBr+Br^-$, noting this reaction likely close to the diffusion limit. Our value of k^{II} for HOBr+Cl- at low acidity ($=(k_1.k_0)/(k_0+k_{-1})$) is a similar order of magnitude to the k^{II} estimate for $HOCl+Cl^-$ (≤ 0.16 M^{-1} s^{-1}, see Gerritsen and Margarem, 1989) or perhaps slightly higher (because the less electronegative Br of HOBr may be more susceptible to nucleophilic attach than HOCl), but is substantially less than the k^{II} estimate for $HOBr+Br^-$ (10^4 M^{-1} s^{-1}, Eigen and Kustin, 1962) at low acidity, and consistent with Cl- being a weaker nucleophile than Br-. Overall, a value for the low acidity k^{II} rate constant; $(k_0\cdot k_1)/(k_1+k_{-1}) = 10^1$ M^{-1} s^{-1} seems reasonable.

A similar analysis based on the three-body rate constant of $2.3\cdot10^{10}$ M^{-2} s^{-1} (Liu and Magarem, 2002). yileds $k_0 = 2\cdot10^1$ s^{-1} and $k_{-1} = 1.1\cdot10^4$ s^{-1}. These estimates for the underlying rate constants for

HOBr+Cl- are rather uncertain, nevertheless the most important result is the occurrence of acid-saturation of k^{II} for HOBr+Cl^-, which the experimental data limits k^{II} to ~10^4 M s^{-1} at pH ≤ 6.

3.3 A new parameterisation for the k^{II} for HOBr+Br^- and HOBr+Cl^-

The underlying rate constants (k_1, k_{-1}, k_H, k_0) for reaction of HOBr+Br^- and HOBr+Cl^- estimated above are summarized in Table 3. Our parameterisation for k^{II} based on these data, with k^{II} defined by equation E6 is shown in Figure 1 as a function of aerosol acidity, alongside the experimental values for k^{II} derived from the reported experimental data from Eigen and Kustin (1962), Beckwith et al. (1996), Liu and Margarem (2001) and Pratte and Rossi (2006) (see Table 2). As expected, the k^{II} parameterisations for HOBr+Br- and HOBr+Cl- exhibit three distinct regimes: k^{II} is independent of acidity at high pH. k^{II} is dependent on acidity for a medium pH range, where the rate constant k^{II} = kter·[$H^+_{(aq)}$], and in this regime the rate constant is termolecular. At high acidity, k^{II} becomes acid-independent (k^{II} = k_1), yielding an acid-saturated k^{II} that is lower for HOBr+Cl- than HOBr+Br- given the weaker nucleophile strength.

Also shown in Figure 1 is the termolecular approach to HOBr kinetics assumed to date, which predicts acid-dependent k^{II} over all parameter space. Clearly, the termolecular assumption for HOBr kinetics is only valid in the termolecular regime, between pH 1-6 for HOBr+Br^-, and > pH 6 for HOBr+Cl^-. At high acidity, the termolecular approach overestimates the rate constant compared to the k^{II} parameterisation by several orders of magnitude. The disagreement is greatest for HOBr+Cl^-, where the termolecular approach overestimates the k^{II} rate constant by a factor of 10^3 at pH = 3 and 10^6 at pH = 0). Of interest is the effect of our revised parameterisation on the HOBr reactive uptake coefficient. Below we compare the reactive uptake coefficients of HOBr calculated our revised k^{II} parameterisation to experimental uptake coefficients reported under laboratory conditions. In section 5 we present calculations of the HOBr reactive uptake coefficient for marine and volcanic plume conditions and discuss implications for reactive halogen chemistry in these environments.

3.4 Comparison of our model with experimental uptake coefficient data

As discussed in the introduction, discrepancies exist in the reported reactive uptake coefficients for HOBr on acidified sea-salt aerosol. Abbatt and Waschewsky (1998) observed a strong pH dependence of the uptake onto sodium chloride aerosol, being $1.5 \cdot 10^{-3}$ for neutral, unbuffered sodium chloride aerosol, rising to > 0.2 for aerosols acidified to pH 0.3 by the addition of HCl, i.e.

close to the accommodation coefficient (α = 0.6 ±0.2, Wachsmuth et al., 2002). The role of H^+ species in the reactive uptake process was further demonstrated by the high uptake coefficient of > 0.2 on aerosols buffered to pH 7 by a NaH_2PO_4 / Na_2HPO_4 buffer. In contrast, Pratte and Rossi (2006) measured reactive uptake coefficients on H_2SO_4-acidified sea-salt aerosol to be ~10^{-2} at H_2SO_4:NaCl = 1.45:1, with an RH-dependence (finding $\gamma_{HOBr} \sim 10^{-3}$ at RH < 70%).

We have calculated the reactive uptake coefficients for HOBr for the conditions of these two laboratory experiments using our new parameterisation for k^{II} and the E-AIM model to determine aerosol composition.

Below we show that the origin for this wide discrepancy between measured HOBr uptake onto acidified bromide aerosol and chloride aerosol lies partly in the difference in reactivity of HOBr towards Br^- and Cl^-, but also in differences in aerosol composition in the two studies: HCl-acidified sea-salt aerosol retains high $Cl^-_{(aq)}$ concentrations, whereas H_2SO_4-acidified sea-salt aerosol undergoes HCl-displacement, lowering $Cl^-_{(aq)}$ concentrations. This acid-displacement of HCl leads to a lowering of the reactive uptake coefficient for HOBr on H_2SO_4-acidified aerosol.

3.4.1 High uptake coefficient on HCl-acidified sea-salt aerosol

On HCl-acidified $NaCl_{(aq)}$ aerosol, Abbatt and Wachewsky (1998) measured the uptake coefficient of HOBr to be > 0.2. We calculate the uptake coefficient for HOBr+Cl^- under these experimental conditions for which a chloride concentration of 6.6 M is predicted according to E-AIM (see details in Section 3.1.1 of Supplementary Material and Table 4). For particles of 1 µm radius at 298 K, both our new parameterisation for k^{II} and the termolecular approach to HOBr+Cl^- kinetics yield high uptake coefficient, $\gamma_{HOBr+Cl}$~0.6, thus are consistent with the experimental findings, see Table 4.

3.4.2 Low uptake coefficient on H_2SO_4-acidified sea-salt aerosol with RH dependence

On H_2SO_4-acidified sea-salt aerosol, Pratte and Rossi (2006) measured the uptake coefficient of HOBr to be ~10^{-2} at H_2SO_4:NaCl = 1.45:1, with an RH-dependence (finding $\gamma_{HOBr} \sim 10^{-3}$ at RH < 70%). Using our parameterisation, we calculate the uptake coefficient for HOBr+Cl- under these experimental conditions, at 298 K, and with variable RH (see details in Section 3.1.2 of Supplementary Material and Table 4). We assume a solubility of HOBr in sulphuric acid of 363 M atm^{-1} at 296 K (following Pratte and Rossi, 2006 based on Iraci et al. 2005), and calculate a HOBr diffusion coefficient in sulphuric acid of $5.5 \cdot 10^{-6}$ cm^2 s^{-1} and $1.0 \cdot 10^{-5}$ cm^2 s^{-1} at 50 and 80 % RH (48 and 29 wt%H_2SO_4)

respectively. E-AIM predicts the aerosol $Cl^-_{(aq)}$ concentrations to be 0.004 M L^{-1} and 0.08 M L^{-1} at 50 and 80 % RH respectively, see Table 4.

The new parameterisation for k^{II} yields uptake coefficients for HOBr+Cl^- of $4.4 \cdot 10^{-3}$ at 50% RH and $7.6 \cdot 10^{-2}$ at 80% RH, in broad agreement to the low uptake coefficients reported by Pratte and Rossi (2006); 1.0 ± 10^{-2} at RH ≥ 76%. Such agreement is to some extent not surprising, given the usage of k^I reported at RH = 77-90% from the same Pratte and Rossi (2006) experiments to derive an estimate for k^{II} at acid saturation (see Section 3 and Figure 1). Nevertheless, the uptake calculations confirm and provide a first explanation for the RH dependence of the uptake coefficient as reported by Pratte and Rossi (2006). The model indicates that the underlying cause of this trend is greater $[Cl^-_{(aq)}]$ at higher RH, given higher solubility of HCl at the lower wt%H_2SO_4 at high RH. This is further shown by Figure 2 that compares the modelled and observed RH dependence of the uptake coefficient of HOBr across all reported data from 40 – 90 % RH, demonstrating broad agreement in the trend (noting discrepancies may result from impurities within the sea-salt solution or uncertainties within the parameterisations used in the uptake model). These findings are in contrast to the termolecular approach to k^I that yields an uptake coefficient of 0.6 at both RH values, substantially overestimating γ_{HOBr} by at least a factor of 20 (see Table 4). This is because the termolecular approach assumes acid-dependent k^{II} across all pH, leading to an extremely high rate constant for the reaction of HOBr+Cl- at pH –1 to 0, and a very fast rate of reaction of HOBr with Cl^-: even though Cl^- concentrations are depleted by acid-displacement, the assumed increased rate constant at low pH overcompensates for this effect.

In conclusion, our new k^{II} parameterisation for the kinetics of HOBr+X- yields uptake coefficients in agreement with reported laboratory data, and -for the first time- reconciles differences between reported uptake on HCl-acidified and H_2SO_4-acidified sea-salt aerosols, within a single framework.

4 Implications for BrO chemistry in the marine and volcanic environments

4.1 Declining uptake coefficients on progressively H_2SO_4-acidified sea-salt aerosol

Using the revised HOBr reaction kinetics (Figure 1), the HOBr+Br- and HOBr+Cl- reactive uptake coefficients are now re-evaluated for a model sea-salt aerosol that undergoes progressive H_2SO_4-acidification (Figure 3) and compared to calculations using the termolecular approach. We investigate how the reductions in halide ion concentrations caused by the $H_2SO_{4(aq)}$ addition (through both acid-displacement reactions that deplete $[Cl^-_{(aq)}]$, and dilution of $[Br^-_{(aq)}]$ by $H_2SO_{4(aq)}$ volume) impact γ_{HOBr} at low pH.

A particle radius of 1 or 0.1 μm is assumed in the uptake calculation. Temperature is set to 298 K and RH = 80% (above deliquescence). For aerosol that is alkaline or only weakly acidic (pH 12 to pH 4), uptake coefficients were calculated assuming a fixed sea-salt composition with $[Cl^-_{(aq)}]$ = 5.3 Mol L^{-1} and $[Br^-_{(aq)}]$ = 0.008 Mol L^{-1}, with pH varied between 4 and 12 (E-AIM was not used given very low degree of H_2SO_4-acidification). For more strongly acidified sea-salt, across H_2SO_4:Na ratios from 0.05 to 400 (pH 4 to -0.87 for the model aerosol conditions), E-AIM was used to determine the extent of acid-displacement of HCl from acidified $NaCl_{(aq)}$ aerosol, with aerosol $Br^-_{(aq)}$ determined using an effective Henry's law solubility for HBr (see predicted composition in Supp. Material Section 3.2).

Figure 4 shows the calculated reactive uptake for HOBr+Br- and HOBr+Cl- increase with increasing acidity over pH 4-12 for the uptake coefficient for 0.1 and 1 μm radius particles, similar to that previously reported using the termolecular approach. The alkaline to acid transition in γ_{HOBr} reflects the increase in the underlying $HOBr_{(aq)}$ k^I rate constant with acidity due to the onset of the acid assisted mechanism, Figure 1 as well as the decrease of HOBr partitioning to BrO^-. $\gamma_{HOBr+Cl}$ reaches values close to the accommodation limit by pH ≤ 8 (for 1 μm radius particles) or pH ≤ 7 (for 0.1 μm radius particles) while $\gamma_{HOBr+Br}$ reaches values close to the accommodation limit by pH ≤ 5 (for 1 μm radius particles) or pH ≤ 4 (for 0.1 μm radius particles).

In the high acidity regime, the acid-saturation of k^{II} can cause γ_{HOBr} to plateau at a level slightly lower than α_{HOBr} (e.g. in $\gamma_{HOBr+Cl}$ at pH ~4), in contrast to the termolecular approach. Overall, for slightly-acidified sea-salt aerosol, reactive uptake of HOBr is driven primarily by $\gamma_{HOBr+Cl}$. $\gamma_{HOBr+Br}$ reaches similar values to $\gamma_{HOBr+Cl}$ at pH ~3-4 for the specific model aerosol conditions of this study.

However, as the degree acidification by H_2SO_4 increases, the uptake coefficient for $HOBr+Cl^-$ begins to decline at pH < 4. This is due to acid-displacement reactions that convert $Cl^-_{(aq)}$ into $HCl_{(g)}$, thereby lowering $[Cl^-_{(aq)}]$. This leads to $\gamma_{HOBr+Cl-} < \gamma_{HOBr+Br-}$, i.e. HOBr reactive uptake becomes driven by HOBr+Br- below a pH of ~2 for the specific aerosol conditions of this study. As H_2SO_4:Na ratio increases further and pH decreases further, the uptake coefficient for $HOBr+Br^-_{(aq)}$ also begins to decline. This is principally due to the dilution of $Br^-_{(aq)}$ by the additional volume of $H_2SO_{4(aq)}$ that becomes important particularly at very high H_2SO_4:Na (see E-AIM calculations in Supplementary Materials).

Notably, the declines in uptake coefficients are greatest for smaller particles, for which there is a greater probability that $HOBr_{(aq)}$ may diffuse across the particle and be released to the gas phase, without any aqueous-phase reaction occurring.

The uptake coefficients are also further reduced if parameterisations for the solubility of HOBr in $H_2SO_{4(aq)}$ is assumed in the uptake equation rather than that for water. The exact point of transition between these two parameterisations is not well constrained, but it is clear that the $H_2SO_{4(aq)}$ parameterisations become more applicable than water with greater acidification, and must certainly be more relevant at high H_2SO_4:Na. The lower solubility of HOBr in $H_2SO_{4(aq)}$ acts to decrease the uptake coefficient, and is found to have a stronger impact on γ_{HOBr} than the slower rate of diffusion of $HOBr_{(aq)}$ in H_2SO_4.

In summary, following a rise over the alkaline-acid transition, our revised HOBr kinetics yields HOBr reactive uptake coefficients that subsequently decline on progressively H_2SO_4-acidified sea-salt aerosol. For the aerosol concentration assumed, the uptake coefficient on the 0.1 μm radius particles declines to $\gamma_{HOBr+Br} < 0.03$ at a H_2SO_4:Na ratio of 400:1, indicating that the reactive uptake of HOBr on highly acidified sub-micrometer particles is extremely low, Figure 3. These decreases in uptake coefficient with increasing aerosol acidity are not captured by calculations that assume termolecular kinetics. As stated in the previous section, this is because the termolecular approach assumes the HOBr rate constant is acid-dependent across all pH, and does not consider acid-saturation of the rate constant.

4.2 Implications for BrO chemistry in the marine boundary layer

Figure 4 shows clearly that higher acidity does not necessarily lead to faster production of reactive bromine. It is well-known that acidity is required for reactive bromine formation to occur: $H^+_{(aq)}$ is consumed in the reaction, therefore a source of acidity is required to sustain prolonged BrO formation chemistry. Further, under alkaline conditions HOBr dissociates into less reactive OBr-. However, the γ_{HOBr} dependency on acidity shown here suggests that additional aerosol acidification by $H_2SO_{4(aq)}$ can act as a limitation to the formation of reactive bromine via HOBr uptake, particularly for small particle sizes.

This leads to the following implications for BrO chemistry in the marine environment, where both supra-micron and sub-micron particles are reported, the former typically being moderately acidified perhaps with some Cl-depletion, and the latter being dominated by H_2SO_4 with only a trace quantity of sea-salt (e.g. Keene et al., 2002):

Firstly, the reactive uptake of HOBr is driven by reaction with Br^- as $\gamma_{HOBr+Cl}$ is reduced on H_2SO_4-acidified (Cl^--depleted) sea-salt aerosol. This leads to a negative feedback in the uptake coefficient for HOBr with BrO chemistry evolution over time, as the conversion of $Br^-_{(aq)}$ to $Br_{2(g)}$ acts to decrease

aerosol [$Br^-_{(aq)}$], reducing subsequent values of $\gamma_{HOBr+Br}$. This negative feedback for $\gamma_{HOBr+Br}$ will play a much more significant role for overall HOBr reactive uptake according our revised HOBr kinetics than has been assumed by model studies to date based on the termolecular approach (for which $\gamma_{HOBr+Cl} \geq \gamma_{HOBr+Cl}$).

Secondly, very low reactive uptake coefficients for both HOBr+Br- and HOBr+Cl- are predicted for sub-micron particles at high H_2SO_4:Na ratios (e.g. $\gamma_{HOBr} < 0.03$, see Figure 4). Such low γ_{HOBr} is proposed as a first explanation for the absence of observable $Br^-_{(aq)}$ depletion in sub-micron $H_2SO_4^-$ dominated particles in the marine environment, in contrast to supra-micron particles where $Br^-_{(aq)}$ depletion is observed and interpreted as evidence of HOBr reactive uptake to form reactive bromine (Sander et al., 2003). Indeed, observations find the submicron H_2SO_4-dominated aerosol to be enriched in $Br^-_{(aq)}$ relative to expected concentrations based on the particle Na^+ content (Sander et al., 2003). A plausible explanation is that the release of $Br_{2(g)}$ from the supra-micron particles leads to the continual formation of gas-phase reactive bromine species of which a proportion will ultimately be deposited back to (both types of) marine aerosols as a source of $Br^-_{(aq)}$. The net effect is for $Br^-_{(aq)}$ concentrations to become enhanced (relative to Na) in the sub-micron aerosol where γ_{HOBr} is low simultaneous to becoming depleted in the supra-micron aerosol where γ_{HOBr} is high. For the former, an upper limit must exist to the extent Br-enrichment can occur whilst maintaining the relatively low $\gamma_{HOBr+Br^-}$. Importantly, this argumentation is only possible using our new uptake calculations based on k^I calculated using revised HOBr kinetics in terms of k^{II}, as the termolecular approach predicts high HOBr reactive uptake for both particle types. We encourage our new rate constants calculations for HOBr reactive uptake to be incorporated into numerical models to test and quantify potential submicron aerosol Br^- enrichment via this proposed mechanism.

We further suggest both of the abovementioned factors may also contribute underlying reasons for the reported over-prediction by numerical models of BrO cycling in the marine environment (Sander et al., 2003; Smoydzin and von Glasow, 2007; Keene et al., 2009). Inclusion of the new HOBr kinetics into such models will allow this hypothesis to be tested and quantified.

4.3 Reactive uptake of HOBr on volcanic aerosol

HOBr reactive uptake coefficients are now calculated for the first time onto aerosol in a halogen-rich volcano plume, using the k^{II} parameterisations for $HOBr+Br^-$ and $HOBr+Cl^-$. Using the volcanic aerosol composition predicted by E-AIM (based on Etna emission scenario, see section 3.3 of Supplementary Material), uptake coefficients for $HOBr+Br^-$ and $HOBr+Cl^-$ are calculated across tropospheric

497 temperature and relative humidity, for two plume dilutions (30 and 0.3 µmol/m^3, which are
498 equivalent to ~1 ppmv, and 0.01 ppmv SO_2 at 4 km altitude in US standard atmosphere), and
499 assuming a particle radius of 1 µm, Figure 4. There exists no experimental information regarding the
500 temperature dependence of k^{II} for HOBr+X. Here it is assumed the variation k^{II} with temperature
501 over 230-300 K is small compared to the temperature dependence of the HOBr and HX solubilities
502 (which vary by several orders of magnitude over the parameter space).

503 High HOBr uptake coefficients are predicted at low tropospheric temperatures: $\gamma_{HOBr+Br^-} \approx \gamma_{HOBr+Cl^-} \approx$
504 0.6. The uptake coefficient decreases markedly with increasing temperature for $\gamma_{HOBr+Cl^-}$ and also
505 decreases for $\gamma_{HOBr+Br^-}$ in the most dilute plume scenario. The inverse temperature trend in γ_{HOBr} is
506 caused by a lower solubility of HX in sulphuric acid particles at higher tropospheric temperatures
507 (particularly for HCl), augmented by a similar temperature trend in the solubility of $HOBr_{(aq)}$. The
508 variation with plume dilution is explained by the fact that lower gas-to-aerosol partitioning yields
509 lower $[X^-_{(aq)}]$ in the dilute plume scenarios thus a lower $k^I = k^{II} \cdot [X^-_{(aq)}]$ in the uptake equation, hence a
510 reduced γ_{HOBr}. Figure 4 also illustrates a weak dependence of the uptake coefficients on relative
511 humidity. This is due to increasing solubility of the halides with RH or lower wt%H_2SO_4 (potential RH-
512 dependence of HOBr solubility is not considered in the parameterisations, see Supplementary
513 Material). As for the marine aerosol study, reductions in γ_{HOBr} are more pronounced for particles of
514 smaller radii (data not shown), as the probability for diffusion across the particle without reaction is
515 higher. According to Figure 4, $\gamma_{HOBr+Br^-}$ is equal to or exceeds $\gamma_{HOBr+Cl^-}$ under all temperature and
516 humidity scenarios for the composition of the Etna emission. This is driven by higher k^I in the uptake
517 calculation (where $k^I = k^{II} \cdot [X^-]$ with k^{II} a function of pH), due to the greater saturation value k^{II} for
518 $HOBr+Br^-$ at high acidity, and the higher solubility of HBr compared to HCl. Again it is important to
519 note that this uptake re-evaluation using revised HOBr kinetics differs from that calculated using the
520 termolecular approach (also shown in Figure 4) which yields high and typically accommodation
521 limited HOBr uptake coefficients throughout the parameter space. Indeed, this is due to the fact that
522 with the termolecular approach ($k^I = k_{ter} \cdot [H^+_{(aq)}] \cdot [X^-_{(aq)}]$) the increased value of k_{ter} at high acidity more
523 than compensates for the acidity-driven decreases in X-, thus yielding high k^I and high γ_{HOBr}.

524

525 Figure 4 shows that in concentrated plumes near to the volcanic source, the aqueous-phase halide
526 concentrations are sufficiently high that $\gamma_{HOBr+Br^-}$ is accommodation-limited. Rapid formation of BrO is
527 expected to occur. This is consistent with observations of volcanic BrO at numerous volcanoes
528 globally (e.g. Bobrowski et al., 2007b, Boichu et al., 2011, and references therein), including
529 emissions from both low and high altitude volcanoes, explosive eruptions and from passive

degassing. However, it is anticipated that the reactive uptake coefficient for HOBr+Br- will be reduced as BrO chemistry progresses causing $Br^-_{(aq)}$ concentrations to decline (due to conversion of HBr into reactive bromine). This will likely slow the BrO cycling in the more evolved plume. Plumes will also become more dilute over time due to dispersion. Figure 4 predicts this will lead to a reduction in the HOBr reactive uptake coefficient particularly in plumes confined to the lower troposphere, which may contribute to a slower rate of BrO cycling. For plumes in the mid-upper troposphere, γ_{HOBr} is predicted to remain high.

To date, numerical model studies of the impacts of volcanic halogens reactive halogen chemistry in the troposphere have either used a fixed uptake coefficient (Roberts et al., 2009; 2014, Kelly et al., 2013) or the termolecular approach to HOBr kinetics (Bobrowski et al., 2009; von Glasow, 2010). Figure 4 illustrates both of these approaches will lead to modelling inaccuracies, particularly in the downwind plume. Incorporation of more realistic HOBr kinetics in these models, using the parameterisations proposed here, is recommended in order to accurately simulate the reactive bromine chemistry and plume impacts.

5 Conclusions

This study introduces a new evaluation of HOBr reactive uptake coefficients on aerosol of different compositions, in the context of the general acid assisted mechanism. We emphasise that the termolecular kinetic approach assumed in numerical model studies of tropospheric reactive bromine chemistry to date is strictly only valid for a specific pH range. Rather, according to the general acid assisted mechanism, the reaction kinetics for HOBr becomes independent of pH at high acidity. By re-evaluation of reported rate constant data from uptake experiments on acidified sea-salt aerosol, and consideration of relative reaction rates according to nucleophile strength, we identify the kinetics of $HOBr+Cl^-$ may saturate below pH 6 to yield a second-order rate constant of $k^{II} \sim 10^4$ M s^{-1}. The kinetics of $HOBr+Br^-$ saturates at $k^{II} \sim 10^8$-10^9 M s^{-1} at pH < ~1 based on experimental data and kinetics estimates of Eigen and Kustin (1962) and Beckwith et al. (1996).

This study reconciles for the first time the different reported uptake reactive coefficient from laboratory experiments. The new k^{II} parameterisation yields uptake coefficients that are consistent with reported uptake experiments: γ_{HOBr} = 0.6 on super-saturated NaBr aerosol (Wachsmuth et al.2002); γ_{HOBr} > 0.2 on HCl-acidfied sea-salt aerosol (Abbatt and Wachsewsky 1998), $\gamma_{HOBr} = 10^{-2}$ on H_2SO_4-acidifed sea-salt aerosol, with an RH dependence (Pratte and Rossi, 2006). The variation in uptake coefficient across the alkaline-aerosol transition is similar to that previously predicted using

the termolecular approach but uptake calculations using our revised kinetics of HOBr show much lower uptake coefficients for HOBr in highly acidified sea-salt aerosol, particularly for small particle radii. This is due to acid-displacement of $HCl_{(g)}$ at high acidity slowing the rate of reaction of HOBr+Cl^-, thus lowering $\gamma_{HOBr+Cl}$, with dilution of $[Br^-_{(aq)}]$ at very high H_2SO_4:sea-salt ratios slowing the rate of reaction of HOBr+Br^-, thus lowering $\gamma_{HOBr+Br}$. This finding contrasts to the existing termolecular approach to uptake calculations in which the higher rate constant overcompensates for the decrease in halide concentration with increasing acidity. Thus, the termolecular approach, as currently used in numerical models of tropospheric BrO chemistry, may cause HOBr reactive uptake to be substantially over estimated in aerosol at high acidity.

Implications for BrO chemistry in the marine boundary layer have been discussed. Firstly, the HOBr uptake coefficient is predicted to be high on slightly acidified supra-micron particles but extremely low on highly-acidified sub-micron particles. A first explanation for the observed Br-enrichment in the sub-micron particles simultaneous to Br-depletion in supra-micron particles is thereby proposed, as reactive bromine release from the supra-micron fraction may deposit and accumulate in the submicron fraction, that does not undergo significant Br- depletion. Secondly, because the HOBr+Br- uptake coefficient is a function of $Br^-_{(aq)}$ concentrations, a negative feedback can occur as the marine BrO chemistry evolves, and supramicron particle $Br^-_{(aq)}$ concentrations are lowered by the release of reactive bromine. According to our revised HOBr kinetics (yielding $\gamma_{HOBr+Br-} > \gamma_{HOBr+Cl-}$), this negative feedback for $\gamma_{HOBr+Br-}$ exerts a stronger overall influence on the rate of HOBr reactive uptake than previous studies have assumed.

Calculations on volcanic aerosol show that uptake is high and accommodation limited in the concentrated near-source plume, enabling BrO formation to rapidly occur. Uptake coefficients are reduced in more dilute plumes, particularly for HOBr+Cl-, at high temperatures (typical lower tropospheric altitudes), for small particle radii. The findings suggest that HOBr uptake on sulphate aerosol directly emitted from volcanoes can readily promote BrO cycling in plumes throughout the troposphere but that the rate of BrO cycling may be reduced by low uptake coefficients in the dispersed downwind plume, particularly at lower tropospheric altitudes. Inclusion of our revised HOBr reaction kinetics in numerical models of volcanic plume chemistry (or uptake coefficients derived therefrom) is required to accurately predict the impacts of volcanic halogens on the troposphere.

Acknowledgements

TJR and LJ are grateful for funding from LABEX VOLTAIRE (VOLatils- Terre Atmosphère Interactions - Ressources et Environnement) ANR-10-LABX-100-01 (2011-20). PTG acknowledges the ERC for funding.

598 **References**

599 Abbatt J. P. D. and Waschewsky G. C.G.: Heterogeneous Interactions of HOBr, HNO3, O3, and NO2
600 with Deliquescent NaCl Aerosols at Room Temperature, J. Phys. Chem. A, 102, 3719-3725, 1998.

601 Ammann, M., Cox, R. A., Crowley, J.N., Jenkin, M. E., Mellouki, A., Rossi, M. J., Troe, J., and
602 Wallington, T. J.: Evaluated kinetic and photochemical data for atmospheric chemistry: Volume VI –
603 heterogeneous reactions with liquid substrates, Atmos. Chem. Phys., 13, 8045 - 8228, 2013, IUPAC
604 Task Group on Atmospheric Chemical Kinetic Data Evaluation, http://iupac.pole-ether.fr/index.html.

605 Barrie L. A., Bottenheim J. W., Schnell R. C., Crutzen P. J., Rasmussen R. A.: Ozone destruction and
606 photochemical reactions at polar sunrise in the lower Arctic atmosphere, Nature, 334, 138-141,
607 1998.

608 Beckwith R. C., Wang T. X., and Margerum D. W.: Equilibrium and Kinetics of Bromine Hydrolysis,
609 Inorg. Chem., 35, 995-1000, 1996.

610 Blatchley, E. R., R. W. Johnson, J. E. Alleman and W. F. McCoy : Effective Henry's law constants for
611 free chlorine and free bromine, Water Research, 26, 99-106, 1991.

612 Bobrowski, N., Honniger, G., Galle, B. and Platt, U.: Detection of bromine monoxide in a volcanic
613 plume. Nature, 423, 273-276, doi:10.1038/nature01625, 2003.

614 Bobrowski, N., von Glasow, R., Aiuppa, A., Inguaggiato, S., Louban, I., Ibrahim, O. W. and Platt, U.:
615 Reactive halogen chemistry in volcanic plumes, J. Geophys. Res., 112, D06311,
616 doi:101029/2006JD007206, 2007a.

617 Bobrowski, N. and Platt, U.: SO_2/BrO ratios studied in five volcanic plumes. J.Volcanol. Geoth. Res.,
618 166, 3-4, 147-160, 10.1016/j.jvolgeores.2007.07.003, 2007b.

619 Boichu, M., Oppenheimer C., Roberts T. J., Tsanev V., Kyle P. R.: On bromine, nitrogen oxides and
620 ozone depletion in the tropospheric plume of Erebus volcano (Antarctica), Atmos. Environ., 45, 23,
621 3856-3866, 2011.

622 Breider T. J., Chipperfield M. P., Richards N. A. D., Carslaw K. S., Mann G. W., Spracklen D. V.: Impact
623 of BrO on dimethylsulfide in the remote marine boundary layer, Geophys. Res. Lett., 37, L02807,
624 doi:10.1029/2009GL040868., 2010.

625 Carslaw K. S., Clegg S. L. and Brimblecombe P.: A thermodynamic model of the system HCl - HNO3 -
626 H2SO4 - H2O, including solubilities of HBr, from <200 K to 328 K. J. Phys. Chem. 99, 11557-11574,
627 1995.

628 Clegg S. L., Brimblecombe P. and Wexler A. S., A thermodynamic model of the system H^+ - NH_4^+ - Na^+
629 - SO_4^{2-} - NO_3^- - Cl^- - H_2O at 298.15 K. J. Phys. Chem. A 102, 2155-2171, 1998.

630 Eigen M. and Kustin K.: The Kinetics of Halogen Hydrolysis, J. Am. Chem. Soc., 1962, 84 (8), pp 1355–
631 1361, DOI: 10.1021/ja00867a005, 1962.

632 Fickert S., Adams J. W. and Crowley J. N.: Activation of Br2 and BrCl via uptake of HOBr onto aqueous
633 salt solutions, Journal of Geophysical Research, 104, D19, 23719-23727, 1999.

634 Frenzel A., Scheer V., Sikorski R., George Ch., Behnke W., and Zetzsch C.: Heterogenerous
635 Interconversion Reactions of BrNO2, ClNO2, Br2, and Cl2., J. Phys. Chem. A, 102, 1329-1337, 1998.

636 Gerritsen C.M. and Margarem D. W.: Non-Metal Redox Kinetics: Hypochlorite and Hypochlorous Acid
637 Reactions with Cyanide, Inorg. Chem., 29, 2757-2762, 1990.

638 Iraci L. T., Michelsen R. R., Ashbourn S. F. M., Rammer T. A., and Golden D. M.: Uptake of
639 hypobromous acid (HOBr) by aqueous sulfuric acid solutions: low-temperature solubility and
640 reaction, Atmos. Chem. Phys., 5, 1577–1587, 2005.

641 Liu Q. and Magarem D. W.: Equilibrium and Kinetics of Bromine, Environ. Sci. Technol., 35, 1127-
642 1133, 2001.

643 Keene W.C., Pszenny A.A.P., Maben J.R., and Sander R.: Variation of marine aerosol acidity with
644 particle size, Geophysical research Letters, 29, 7, 1101, 10.1029/2001GL013881, 2002.

645 Keene W. C., Long M. S., Pszenny A. A. P. Sander R., Maben J. R., Wall A. J., O'Halloran T. L., Kerkweg
646 A., Fischer E. V., and Schrem O.: Latitudinal variation in the multiphase chemical processing of
647 inorganic halogens and related species over the eastern North and South Atlantic Oceans, Atmos.
648 Chem. Phys., 9, 7361–7385, 2009.

649 Kelly P J., Kern C., Roberts T. J., Lopez T., Werner C., Aiuppa A., Rapid chemical evolution of
650 tropospheric volcanic emissions from Redoubt Volcano, Alaska, based on observations of ozone and
651 halogen-containing gases, Journal of Volcanology and Geothermal Research, Volume 259, Pages 317-
652 333, 2013.

653 Klassen, J. K., Hu, Z. and Williams, L. R.: Diffusion coefficients for HCl and HBr in 30 wt % to 72 wt %
654 sulfuric acid at temperatures between 220 and 300 K, J. Geophys. Res. 103, 16197-16202, 1998.

655 Kumar K. and Margarem D. W.: Kinetics and Mechanism of General- Acid-Assisted Oxidation of
656 Bromide by Hypochlorite and Hypochlorous Acid, Inorg. Chem. 26, 2706-2711,1987.

Martin R.S.,, Wheeler J.C., Ilyinskaya E., Braban C.F. and Oppenheimer C: The uptake of halogen (HF, HCl, HBr and HI) and nitric (HNO3) acids into acidic sulphate particles in quiescent volcanic plumes, Chemical Geology 296-297, 19–25, 2012.

Nagy J.C., Kumar K., Margarem D. W.: Non-Metal Redox Kinetics: Oxidation of Iodide by Hypochlorous Acid and by Nitrogen Trichloride Measured by the Pulsed-Accelerated-Flow Method, Inorganic Chemistry, Vol. 27, No. 16, 2773-2780, 1988.

Nagy P. and Ashby M.T.: Reactive Sulfur Species: Kinetics and Mechanisms of the Oxidation of Cysteine by Hypohalous Acid to Give Cysteine Sulfenic Acid, J. Am Chem Soc, 129, 14082-14091, 2007.

Parrella J. P., Jacob D. J., Liang Q., Zhang Y., Mickley L. J., Miller B., Evans, M. J., Yang X., Pyle J. A., Theys N., and Van Roozendael M.: Tropospheric bromine chemistry: implications for present and pre-industrial ozone and mercury, Atmos. Chem. Phys., 12, 6723-6740, 2012.

Pratte P. and Rossi M. J.: The heterogeneous kinetics of HOBr and HOCl on acidified sea salt and model aerosol at 40–90% relative humidity and ambient temperature, Physical Chemistry Chemical Physics, 8, 3988–4001, 2006.

Read K. A., Mahajan A. S., Carpenter L. J., Evans M. J., Faria B. V. E., Heard D. E., Hopkins J. R., Lee L. D., Moller S. J., Lewis A. C., Mendes L., McQuaid J. B., Oetjen H., Saiz-Lopez A., Pilling M. J. and Plane J. M. C., Extensive halogen-mediated ozone destruction over the tropical Atlantic Ocean, Nature, 453, doi:10.1038/nature07035, 1232-1235, 2008.

Roberts, T. J., Braban, C. F., Martin, R. S., Oppenheimer, C., Adams, J. W., Cox, R. A., Jones R. L. and Griffiths., P. T, Modelling reactive halogen formation and ozone depletion in volcanic plumes. Chem. Geol., 263,151-163, 2009.

Roberts T.J., Martin R.S, Jourdain L.,: Reactive halogen chemistry in Mt Etna's volcanic plume: the influence of total Br, high temperature processing, aerosol loading and plume dispersion, ACPD, 2014.

Saiz-Lopez A., and von Glaosw R., Reactive halogen chemistry in the troposphere, Chem Soc Rev, 41,6448-6472, 2012.

Sander R., Keen W. C., Pszenny A. A. P., Arimoto R.,Ayers G. P.,Baboukas E., Cainey J. M., Crutzen P. J., Duce R. A., Hönninger G., Huebert B. J., Maenhaut W., Mihalopoulos N., Turekian V. C., and Van Dingenen R.: Inorganic bromine in the marine boundary layer: a critical review, Atmos. Chem. Phys., 3, 1301-1336, 2003.

688 Sander R., Baumgaertner A., Gromov S., Harder H., Jöckel P., Kerkweg A., Kubistan D., Regelin E.,
689 Riede H., Sandu A., Taraborelli D., Tost H. and Xie Z.-Q.: The atmospheric chemistry box model
690 CAABA/MECCA-3.0,Geosci. Model Dev., 4, 373–380, 2011.

691 Sander R., Compilation of Henry's Law Constants for Inorganic and Organic Species of Potential
692 Importance in Environmental Chemistry (Version 3), http://www.henrys-law.org accessed November
693 2013, 1999.

694 Schmodzin L. and von Glasow R.: Do organic surface films on sea salt aerosols influence atmospheric
695 chemistry? – a model study, Atmos. Chem. Phys., 7, 5555-5567, doi:10.5194/acp-7-5555-2007, 2007.

696 Schroeder W.H., Anlauf K. G., Barrie L. A., Lu J. Y., Steffen A., Schneeberger D. R. and Berg T.: Arctic
697 springtime depletion of mercury, Nature, 394, 331-332, doi:10.1038/28530, 1998.

698 Schweizer F., Mirabel P. and George C., Uptake of hydrogen halides by water droplets, J. Phys Chem
699 A., 104, 72-76, 2000.

700 Seinfeld, John H. ; Pandis, Spyros N. Atmospheric Chemistry and Physics - From Air Pollution to
701 Climate Change (2nd Edition). John Wiley & Sons, accessed November 2013, 2006

702 Simpson W.R., von Glasow, R., Riedel K., Anderson P., Ariya P., Bottenheim J., Burrows J., Carpenter
703 L. J., Friess U., Goodsite M. E., Heard D., Hutterh M., Jacobi H.-W., Kaleschke L., Neff B., Plance J.,
704 Platt U., Richter A., Roscoe H., Sander R., Shepson P., Sodeau J., Steffen A., Wagner T., and Wolff E.:
705 Halogens and their role in polar boundary-layer ozone depletion, Atmos. Chem. Phys., 7, 4375–4418,
706 2007.

707 Vogt R., Crutzen P. J., and Sander R.: A mechanism for halogen release from sea-salt aerosol in the
708 remote marine boundary layer, Nature, 383, 327-330, 1996.

709 Von Glasow R. and Sander R.: Variation of sea salt aerosol pH with relative humidity, Geophysical
710 Research Letters, 28, 2, 247-250, 2001.

711 Von Glasow R., Sander R., Bott, A., Crutzen P. J.: Modeling halogen chemistry in the marine boundary
712 layer 1. Cloud-free MBL, Journal of Geophysical Research 107, D17, 4341,
713 doi:10.1029/2001JD000942, 2002.

714 Von Glasow R., von Kuhlmann R., Lawrence M. G., Platt U., and Crutzen P. J.: Impact of reactive
715 bromine chemistry in the troposphere, Atmos. Chem. Phys., 4, 2481-2497, 2004.

716 Von Glasow, R.: Atmospheric Chemistry in Volcanic Plumes, PNAS, 107, 15, 6594-6599, 2010.

717 Wachsmuth M., Gäggeler H. W., von Glasow R., Ammann M. : Accommodation coefficient of HOBr
718 on deliquescent sodium bromide aerosol particles, Atmos. Chem. Phys., 2, 121–131, 2002.

719 Wang T. X. and Margarem D. W.: Kinetics of Reversible Chlorine Hydrolysis: Temperature
720 Dependence and General-Acid/ Base-Assisted Mechanisms, Inorg. Chem., 33, 1050-1055, 1994.

721 Wexler A. S. and Clegg S. L.: Atmospheric aerosol models for systems including the ions H^+, NH_4^+, Na^+,
722 SO_4^{2-}, NO_3^-, Cl^-, Br^- and H_2O. J. Geophys. Res. 107, No. D14, 4207-4220, 2002.

723 Wilson, T.R.S.: Salinity and the major elements of sea water. In: Riley, J.P., Skirrow, G. (Eds.),
724 Chemical Oceanography (1, 2 Edition). Academic, Orlando FL, 365 – 413, 1975.

725 Yang, X., Cox R. A., Warwick N. J., Pyle J. A., Carver G. D., O'Connor F. M., and Savage N. H.:
726 Tropospheric bromine chemistry and its impacts on ozone: A model study, J. Geophys. Res., 110,
727 D23311, doi:10.1029/2005JD006244., 2005.

728

Table 1. Summary of experimental data reported on HOBr uptake coefficient and $HOBr_{(aq)}$ reaction kinetics under tropospheric conditions.

Aerosol or Solution	Temperature K	k_{ter} $M^{-2}\ s^{-1}$	k^{I} s^{-1}	k^{II} $M^{-1}\ s^{-1}$	γ_{HOBr}	α_{HOBr}	Ref.
$HOBr + Cl^-_{(aq)}$							
HCl-acidifed NaCl aerosol with HCl:NaCl = 0.1:1	298	-	-	-	> 0.2	-	[a]
H2SO4-acidified sea-salt aerosol with H_2SO_4:NaCl = 1.45:1	296	-	10^3	-	10^{-3}-10^{-2}	-	[b]
$BrCl_{(aq)}$ solution, pH = 6.4	298	$2.3\cdot10^{10}$	-	-	-	-	[c]
$HOBr+Br^-_{(aq)}$							
HOBr uptake onto supersaturated $NaBr_{(aq)}$, $Br^-_{(aq)}$ > 0.2 M, at very low $[HOBr_{(g)}]$	296 ±2	-	-	-	-	0.6	[d]
$Br_{2(aq)}$ solution, pH = 2.7-3.8	298	$1.6\cdot10^{10}$	-	-	-	-	[e]
$Br_{2(aq)}$ solution, pH = 1.9-2.4	298	$1.6(\pm0.2)\cdot10^{10}$	-	-	-	-	[f]

[a]Abbatt and Waschewsky (1998)
[b]Pratte and Rossi (2006)
[c]Liu and Margarem (2002)
[d]Wachsmuth et al. (2002)
[e]Eigen and Kustin (1962)
[f]Beckwith et al. (1996)

Table 2. Extraction of second-order rate constant values, k^{II} from reported experimental data. For HOBr+Br, k^{II} is derived from reported termolecular rate constants using $k^{II} = k_{ter}\cdot[H^+_{(aq)}]$. For HOBr+Cl- k^{II} is derived from a reported termolecular rate constant using $k^{II} = k_{ter}\cdot[H^+_{(aq)}]$ and from reported first-order rate constant data, k^I using $k^{II} = k^I/[Cl^-_{(aq)}]$. Molarity and Activity of $Cl^-_{(aq)}$ and $H^+_{(aq)}$ were calculated using the E-AIM model at 298.15 K. See Methods.

Experiment	T K	RH %	wt% H_2SO_4	pH	$Cl^-_{(aq)}$ Activity M	k_{ter} $M^{-2}\,s^{-1}$	k^I s^{-1}		k^{II} $M^{-1}\,s^{-1}$		Ref.
HOBr+Br$^-$											
$Br_{2(aq)}$	293	-	-	2.7-3.6	-	$1.6\cdot10^{10}$	-		$4.\cdot10^{6}$ - $3.2\cdot10^{7}$		a
$Br_{2(aq)}$	298	-	-	1.9-2.4	-	$1.6\ (\pm0.2)\cdot10^{10}$	-		$6.1\cdot10^{7}$ - $1.9\cdot10^{8}$		b
HOBr+Cl$^-$											
$BrCl_{(aq)}$	298	-	-	6.4	2.0	$2.3\cdot10^{10}$	-		$8.8\cdot10^{3}$		c
							($\alpha = 0.2^*$)	($\alpha = 0.02^*$)	($\alpha = 0.2^*$)	($\alpha = 0.02^*$)	
H_2SO_4:NaCl (1.45:1)	296	77	31.7	-0.84	0.056		922	1855	$1.6\cdot10^{4}$	$3.3\cdot10^{4}$	d
	296	79	30.00	-0.75	0.069		1050	2510	$1.5\cdot10^{4}$	$3.6\cdot10^{4}$	
	296	80	29.1	-0.71	0.076		1140	3010	$1.5\cdot10^{4}$	$3.9\cdot10^{4}$	
	296	85	24.2	-0.48	0.127		800	1485	$6.3\cdot10^{3}$	$1.2\cdot10^{4}$	
	296	90	17.7	-0.21	0.209		995	2355	$4.8\cdot10^{3}$	$1.1\cdot10^{4}$	
H_2SO_4:NaCl (1.45:1)NSS	296	77	31.7	-0.84	0.056		1960	44000	$3.5\cdot10^{4}$	$7.8\cdot10^{5}$	d
H_2SO_4:NaCl (1.45:1) RSS	296	77	31.7	-0.84	0.056		545	795	$9.6\cdot10^{3}$	$1.4\cdot10^{4}$	d
	296	79	30.00	-0.75	0.069		720	1225	$1.0\cdot10^{4}$	$1.8\cdot10^{4}$	
	296	80	29.1	-0.71	0.076		1090	2600	$1.4\cdot10^{4}$	$3.4\cdot10^{4}$	
	296	85	24.2	-0.48	0.127		815	1580	$6.4\cdot10^{3}$	$1.2\cdot10^{4}$	
	296	90	17.7	-0.21	0.209		710	1210	$3.4\cdot10^{3}$	$5.8\cdot10^{3}$	

[a]Termolecular rate constant reported by Eigen and Kustin (1962)

[b]Termolecular rate constant reported by Beckwith et al. (1996)

[c]Termolecular rate constant reported by Liu and Magarem (2001) for buffered aerosol containing $Cl^-_{(aq)}$ at pH = 6.4 at T = 298 K.

[d]First-order rate constant, k^I_{rxn} data reported by Pratte and Rossi (2005) for aerosol mixture at H2SO4:NaCl = 1.45, for laboratory sea-salt, natural sea-salt (nss) or recrystalised sea-salt (rss). Pratte and Rossi (2006) assumed two different accommodation coefficients (α= 0.2, α= 0.02) in the derivation of k^I_{rxn} values from their uptake experiments, the former being closest to α= 0.6 reported on $NaBr_{(aq)}$ aerosol by Wachsmuth et al. (2002).

Table 3. Underlying rate constant data (k_1, k_{-1}, k_0, k_H) used in k^{II} parameterisations of Figure 1.

	HOBr+Br	HOBr+Cl
k_1, M^{-1} s^{-1}	$5 \cdot 10^{8}$ [b,a]	$1.2 \cdot 10^{4}$ [c]
k_{-1}, s^{-1}	$5 \cdot 10^{8}$ [b,a]	$1.1 \cdot 10^{4}$ [c]
k_0, s^{-1}	10^{4} [a]	$2 \cdot 10^{1}$ [c]
k_H, M^{-1} s^{-1}	$2 \cdot 10^{10}$ [a]	$2 \cdot 10^{10}$ [c]

a: estimated in this study
b: derived from Eigen and Kustin (1962)
c: derived from Kumar and Margerum (1987)

Table 4 Predicted uptake coefficients compared to reported uptake on experimental aerosol

* Br^- concentration prior to aerosol dehumidifying (reported reduction in volume during dehumidifying indicates actual concentration may be a factor of ~3 higher)

**(reported modal radius, although particles >0.2 µm exist within the size spectrum)

Experimental aerosol:	NaBr aerosol (Wachsmuth et al., 2002) supersaturated $NaBr_{(aq)}$	HCl-acidified NaCl aerosol (Abbatt and Waschewsky, 1998) HCl/NaCl = 0.1:1	H_2SO_4-acidified sea-salt aerosol (Pratte and Rossi, 2006) H_2SO_4/NaCl = 1.45:1	
γ_{HOBr}: observed	0.6 ±0.2	> 0.2	$(0.1\text{-}0.3)\cdot10^{-2}$ at RH 40 to 70 %	$(1.0\pm0.2)\cdot10^{-2}$ at RH ≥ 76 %
Uptake Model Parameters:				
Temperature	298.15	298.15	298.15	298.15
α (accommodation coefficient)	0.6	0.6	0.6	0.6
Na concentration (µmol/m^3)	-	0.2	0.8	0.8
RH, %	80	76	50	80
$[Br^-_{(aq)}]$, M	> 0.2*	-	-	-
$[Cl^-_{(aq)}]$, M (E-AIM)	-	6.6	$4.4\cdot10^{-3}$	$7.6\cdot10^{-2}$
$[H^+_{(aq)}]$, M (E-AIM)	$\sim2\cdot10^{-6}$	2.3	83	5
pH	~6	-0.3	-1.9	-0.7
k^{II}, M^{-1} s^{-1}	$3\cdot10^4$	10^4	10^4	10^4
k_{ter}, M^{-2} s^{-1}	$1.6\cdot10^{10}$	$2.3\cdot10^{10}$	$2.3\cdot10^{10}$	$2.3\cdot10^{10}$
Particle radius, µm	>0.03**	1.	~0.17	~0.17
wt%H_2SO_4	-	-	48	29
HOBr solubility, M atm^{-1}	$6.1\cdot10^3$	$6.1\cdot10^3$	364	364
HOBr Diffusion constant, cm^2 s^{-1}	$1.42\cdot10^{-5}$	$1.42\cdot10^{-5}$	$5.5\cdot10^{-6}$	$1.0\cdot10^{-5}$
γ_{HOBr}: old approach (where $k^I = k_{ter}\cdot[X^-_{(aq)}]\cdot[H^+_{(aq)}]$)	$0.1 < \gamma_{HOBr} \leq 0.6$	0.6	0.6	0.6
γ_{HOBr}: new approach (where $k^I = k^{II}\cdot[X^-_{(aq)}]$)	$0.1 < \gamma_{HOBr} \leq 0.6$	0.6	$2\cdot10^{-4}$	$7\cdot10^{-3}$

Figure 1

Second order rate constants for the reaction of HOBr with Br^- and Cl^- as a function of pH. Experimental estimates for k^{II} for HOBr+Br^- derived from data from Eigen and Kustin (1962) and Beckwith et al. (1996), (blue squares and circles respectively) are shown alongside model estimate (blue line) according to the acid-assisted mechanism. The red line denotes the k^{II} rate constant assuming termolecular kinetics across all pH. Experimental estimates for k^{II} for HOBr+Cl^- derived from data from Liu and Margarem (2001) at pH = 6.4 (black triangle) and Pratte and Rossi (2006) at pH -1 to 0 (black and grey disks for data at RH = 77-80%, open circles for RH = 85-90%), are shown alongside model estimate (black line) according to the general acid-assisted mechanism. The green line denotes the k^{II} rate constant assuming termolecular kinetics across all pH.

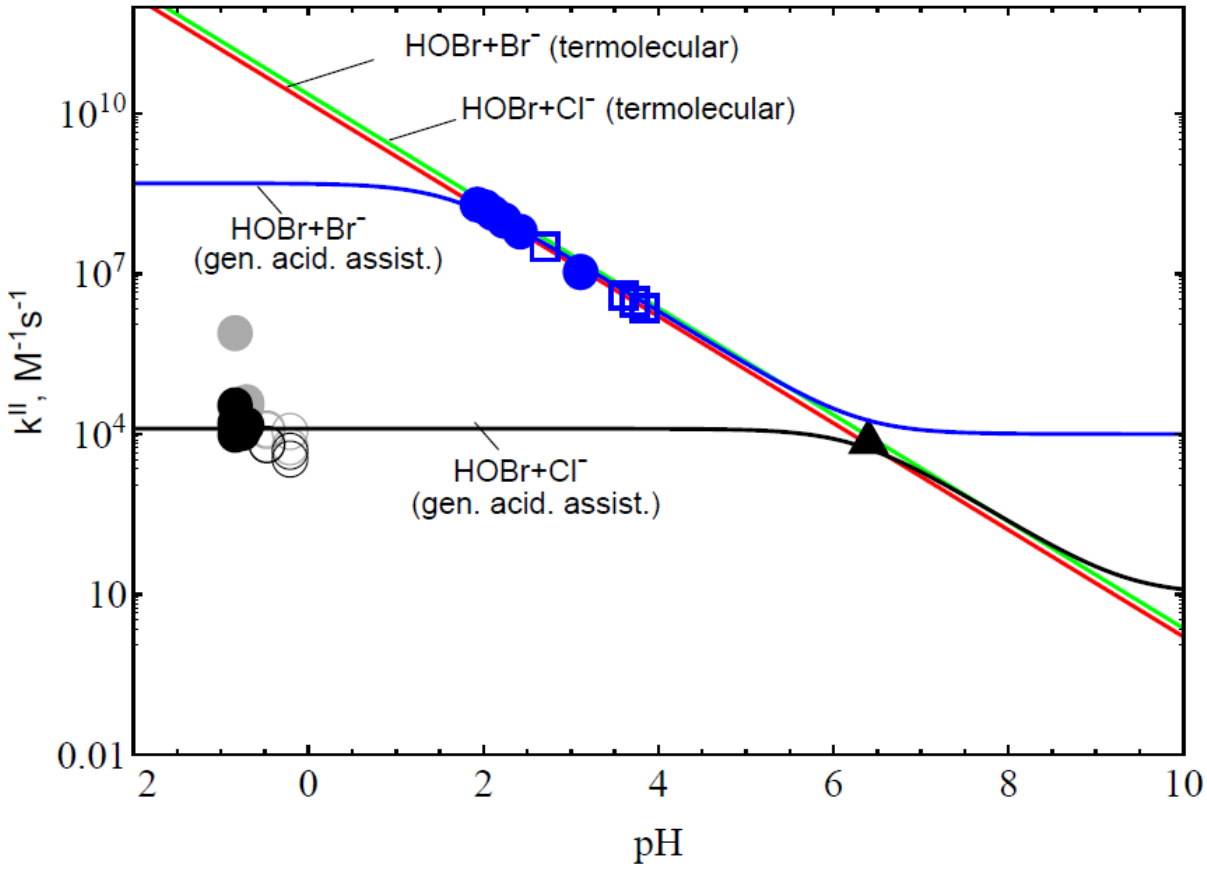

Figure 2

Dependence of reactive uptake coefficient for HOBr on relative humidity (RH) in the experiments of Pratte and Rossi (2006) on H_2SO_4-acidified sea-salt aerosol (H_2SO_4:NaCl = 1.45:1) at 296 K, on acidified sea-salt (circles), recrystallized sea-salt (squares) and natural sea-salt (triangles), under two experimental set-ups: (i) the observed rate of $HOBr_{(g)}$ decay for a measured aerosol size distribution, with effective radius ranging over 165-183 nm (filled shapes), and (ii) a survey type mode with HOBr depletion monitored as a function of RH (unfilled shapes, with reported error estimated at 30-50%) over a constant reaction time. Also shown is the modelled uptake coefficient for HOBr (black line), and the $Cl^-_{(aq)}$ molarity (dotted line) as used within the uptake calculation.

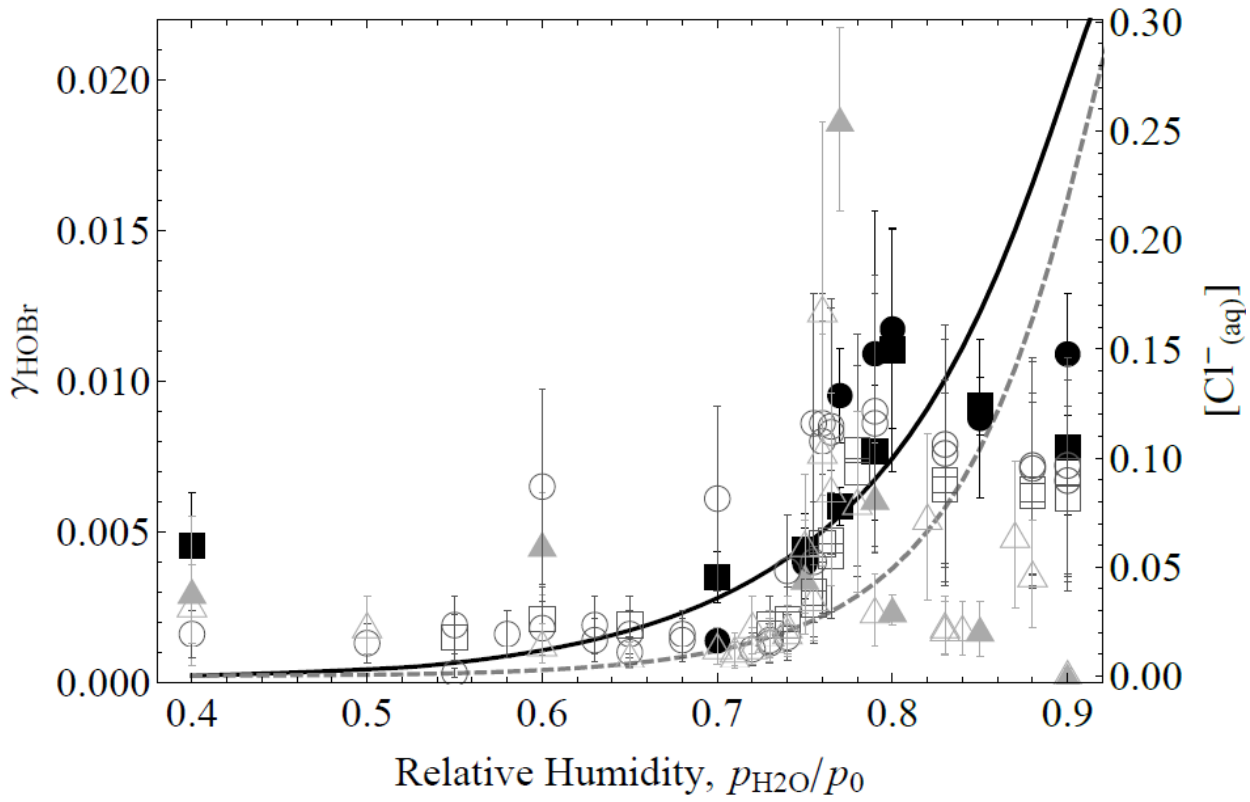

Figure 3

Variation in the HOBr uptake coefficient with pH, for reaction of HOBr with (upper) Cl- and (lower) Br- on H_2SO_4-acidified sea-salt aerosol. Grey and orange lines denote uptake onto 1 and 0.1 µm radius particles, respectively. Black and red lines denote uptake onto 1 and 0.1 µm radius particles calculated using H^* and D_l parameterisations for sulfuric acid (rather than water), shown only for H_2SO_4:Na ratios greater than 0.5. Relative humidity is set to 80% and Na concentration $1.3 \cdot 10^{-7}$ moles/m^3 (equivalent to a PM10 of 10 µg/m^3 in the marine environment, Seinfeld and Pandis, 2006). For comparison, uptake coefficients calculated assuming termolecular kinetics are also shown (dashed lines).

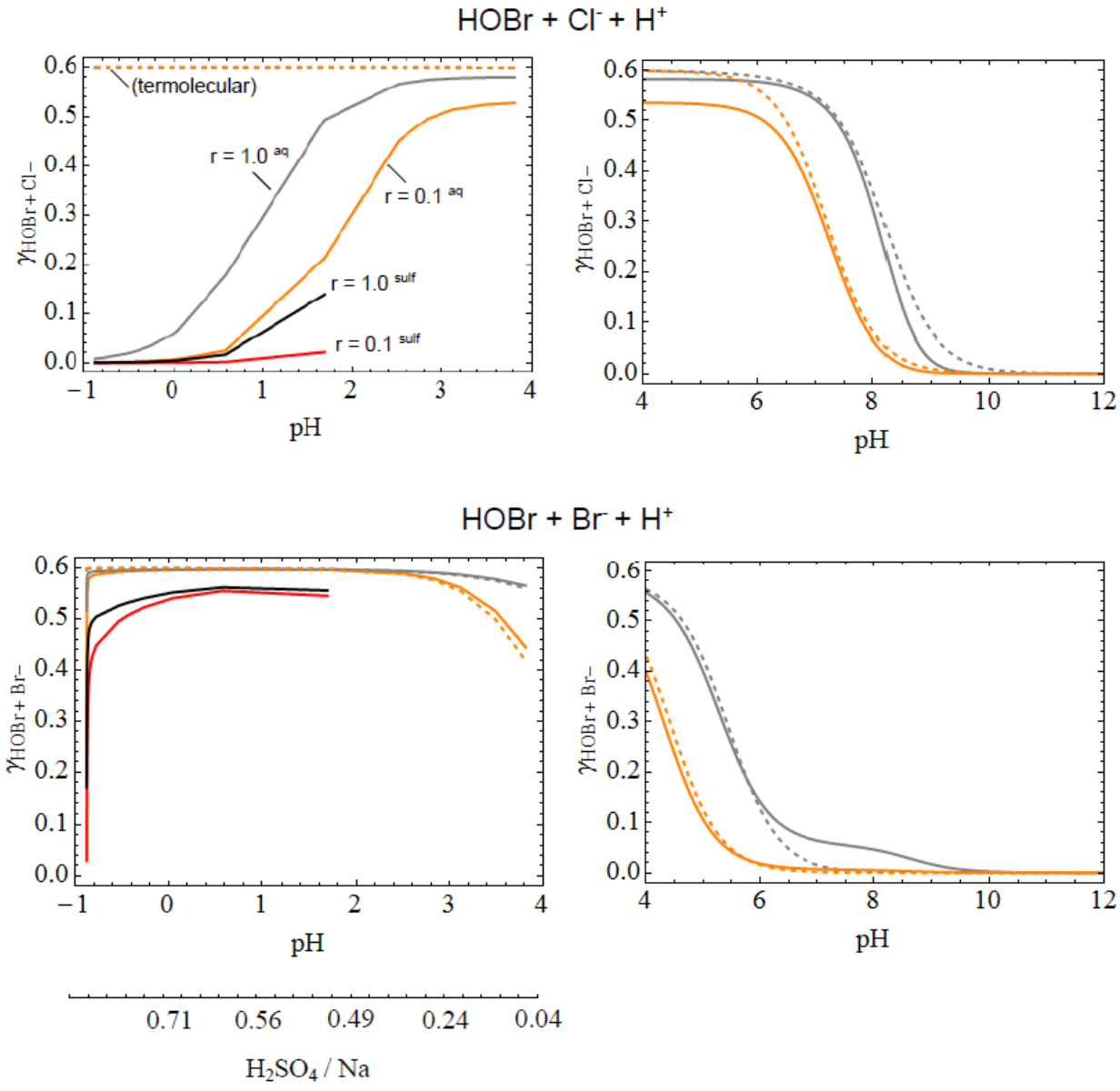

Figure 4

HOBr+Cl- and HOBr+Br- reactive uptake coefficients onto volcanic sulphate aerosol particles of 1 µm radius, calculated using our revised HOBr kinetics. Calculations are performed for a typical Arc or subduction zone volcanic plume composition containing a (SO_2):HCl:H_2SO_4:HBr molar ratio mixture of 1:0.5:0.01:0.00075. The plume strength is 30, or 0.3 µmol/m^3, equivalent to approximately 1 or 0.01 ppmv SO_2 at 4 km altitude (US standard atmosphere). Conversely, uptake coefficients calculated using the termolecular approach yield high accommodation-limited values across all parameter space (light grey).